Electrochimica Acta 187 (2016) 249–255

Contents lists available at ScienceDirect

Electrochimica Acta

journal homepage: www.elsevier.com/locate/electacta

Exploring Graphene Quantum Dots/TiO_2 interface in photoelectrochemical reactions: Solar to fuel conversion

Pitchaimuthu Sudhagar[a,e], Isaac Herraiz-Cardona[b], Hun Park[c], Taesup Song[d], Seung Hyun Noh[c], Sixto Gimenez[b,*], Ivan Mora Sero[b], Francisco Fabregat-Santiago[b], Juan Bisquert[b,f], Chiaki Terashima[e], Ungyu Paik[d], Yong Soo Kang[d,*], Akira Fujishima[e], Tae Hee Han[c,*]

[a] Centre for Next Generation Dye-sensitized Solar Cells, Department of Energy Engineering, Hanyang University, Seoul 133-791, South Korea
[b] Institute of Advanced Materials (INAM), Universitat Jaume I, 12071Castelló, Spain
[c] Department of Energy Engineering and Advanced Materials Science Engineering, Hanyang University, Seoul 133-791, South Korea
[d] Department of Organic and Nano Engineering, Hanyang University, Seoul 133-791, South Korea
[e] Photocatalysis International Research Center, Research Institute for Science & Technology, Tokyo University of Science, 2641 Yamazaki, Noda, Chiba 278-8510, Japan
[f] Department of Chemistry, Faculty of Science, King Abdulaziz University, Jeddah 21589, Saudi Arabia

ARTICLE INFO

Article history:
Received 24 August 2015
Received in revised form 1 October 2015
Accepted 8 November 2015
Available online 12 November 2015

Keywords:
TiO_2
graphene quantum dots
water splitting
solar fuel
photoelectrochemical
charge transfer

ABSTRACT

Photocarrier (e^-/h^+) generation at low dimension graphene quantum dots offers multifunctional applications including bioimaging, optoelectronics and energy conversion devices. In this context, graphene quantum dots onto metal oxide electron transport layer finds great deal of attention in solar light driven photoelectrochemical (PEC) hydrogen fuel generation. The merits of combining tailored optical properties of the graphene quantum dots sensitizer with the transport properties of the host wide band gap one dimensional nanostructured semiconductor provide a platform for high charge collection which promotes catalytic proton reduction into fuel generation at PEC cells. However, understanding the underlying mechanism of photocarrier transfer characteristics at graphene quantum dots/metal oxide interface during operation is often difficult as graphene quantum dots may have a dual role as sensitizer and catalyst. Therefore, exploring photocarrier generation and injection at graphene quantum dot/metal oxide heterointerfaces in contact with hole scavenging electrolyte afford a new pathway in developing graphene quantum dots based photoelectrochemical fuel generation systems. In this work, we demonstrate direct assembly of surface modified graphene quantum dots (~2 nm particle size) onto TiO_2 hollow nanowire (~3 μm in length and ~100 to 250 nm in diameter) by electrostatic attraction and examine the photocarrier accumulation and recombination processes leading to device operation. Optical characterization reveals that GQDs absorbed light photons at visible light wavelength up to 600 nm. Hybrid TiO_2-GQDs heterostructures show a photocurrent enhancement of ~70% for water oxidation compared to pristine TiO_2 using sacrificial-free electrolyte, which is further validated by incident photon to current efficiency. Additionally, the charge accumulation processes and charge transfer characteristics are investigated by electrochemical impedance spectroscopy. These results provide the platform to understand the insights of graphene quantum dots/metal oxide interfaces in PEC reactions and discuss the feasibility of graphene quantum dots in wide range of electrochemical and photoelectrochemical based fuel conversion devices.

1. Introduction

Photoelectrochemical hydrogen generation by water splitting with semiconductor materials constitutes the most attractive approach towards the direct conversion of solar energy into chemical fuels [1]. Since the pioneering report of Fujishima and Honda in 1972 [2], TiO_2 has been intensively studied as the most stable

* Corresponding authors.
E-mail addresses: sjulia@uji.es (S. Gimenez), kangys@hanyang.ac.kr (Y.S. Kang), than@hanyang.ac.kr (T.H. Han).

http://dx.doi.org/10.1016/j.electacta.2015.11.048
0013-4686/

photocatalyst to date. However, the negligible light harvesting efficiency in the visible range of the spectrum constitute a serious drawback of this material for energy conversion applications and extensive exploration of different strategies to enhance the visible absorption of TiO_2 has been carried out in the last 40 years. Doping with interstitial atoms like C [3], N [4] or S [5] has provided limited success in extending the absorption range of TiO_2. Another common approach relies on sensitization with narrow bandgap semiconductors and generally entails the use of chalcogenide materials, (CdS, CdSe, PbS, etc) which pose environmental problems and exhibit fast photocorrosion in aqueous solutions unless a hole scavenger is present in the solution [6–8].

On the other hand, graphene (a 2-dimensional network of hexagonal structured sp^2-hybridized carbon atoms) [9] has emerged in the last years as a novel material with outstanding optoelectronic properties able to revolutionize energy conversion architectures and devices [10,11]. Its high conductivity (10^6 S cm^{-1}), excellent room-temperature mobility of charge carriers ($2 \cdot 10^5$ $cm^2 V^{-1} s^{-1}$), large theoretical specific surface area (2630 $m^2 g^{-1}$) and high optical transmittance (~98%) are some of these unique features [12]. Although graphene is generally considered a zero bandgap semiconductor, its electronic structure can be engineered by heteroatom doping, electrostatic field tuning [13], and size control [14] and a n-type or p-type semiconductor with a small bandgap can be obtained.

One of the interesting approaches to downsize layered graphene [15–17] or graphite [18–20] by top-down methods or carbonizing the organic precursors through bottom-up techniques [21] leads to band gap induced graphene quantum dots (GQDs). Apparently, these zero dimension GQDs show effective photocarrier generation and separation at metal oxide interface compared to graphene layers, which may anticipate reducing the charge recombination rate [22]. During the last few years significant research has been progressed to scale up the GQDs yield in gram scale towards industrial applications [18,23]. Some reports explore the possibility of GQDs synthesis from natural resources of coal [24,25] and plant leafs [26] encouraging the utilization of GQDs in a broad range of device applications at low cost.

The highly conducting behaviour of GQDs is widely implemented as tunnelling gate in gas sensors [27,28], and memory devices [29]. In addition, GQDs serve as intermediate electron acceptor layers in electrochromic displays and solar cells [30,31], which facilitate the charge separation from photoactive layer to electron transport layer. Therefore, the size and edge controlled [32,33] band gap tuneable graphene quantum dots is an appropriate choice in light harvesting agents compare to graphene and can be utilized in multifunctional applications where the photoexcited carriers takes a key role [34,35].

In this line, graphene GQDs have been recognized as a cost-competitive, environmentally benign, and stable photoactive material in a broad range of light driven optoelectronic device applications such as photodetector, photovoltaics, photocatalyst and photoelectrochemical devices [31,36,37]. These reports strongly corroborate that GQDs can access the light photons from wide solar spectrum and can be utilized in electricity or fuel generation. Indeed, aggregation of GQDs [21] in liquid medium could affect their optical properties The assembly of GQDs monolayer onto mesoporous metal oxide electron transport framework [38] shows analogous photosensitizer effect like organic dye molecules or semiconductor quantum dots [39–41]. Comparing to common sensitization strategies, this approach involves environmentally friendly materials and in contrast to metal chalcogenide QDs, the use of hole scavengers is not needed, which greatly maximizes the potential of this material for solar fuels applications.

However, the photoexcited charge carrier separation at GQDs/metal oxide electronic interfaces is less understood, since GQDs can play both photosensitizer and electrocatalyst roles simultaneously at metal oxide host surface, which often leads to problems to recognize their effect. Therefore identifying the underlying mechanism of GQDs under photoirradiation in conjugation with metal oxide nanostructure could be informative to promote the utilization of GQDs in solar to fuel generation process. In this work, we demonstrate the photoelectrochemical reactions at GQDs/TiO_2 hollow nanowire (HNW) architecture electrode and their charge transfer characteristics in the context of solar to fuel conversion. These TiO_2 hollow nanowires appear as promising architectures for solar energy conversion applications, due to the promotion of light scattering effects, which leads to enhanced light harvesting efficiency. More importantly, we correlate the functional performance of the devices with the mechanisms leading to device operation, i.e., charge accumulation and recombination.

2. Experimental

2.1. Materials

Graphite powder was purchased from Asbury carbons (USA, Grade: 2012). Potassium permanganate, hydrogen peroxide, ammonia were purchased from Sigma-Aldrich and sulfuric acid and hydrochloride were obtained from Samchun Chemical. All chemicals were used as received without additional purification. Water was deionized using a Milipore MilliQ® system.

2.2. Synthesis of graphene oxide and graphene quantum dots

Graphene oxide was synthesized from natural graphite by the modified Hummers method, as described elsewhere [42,43]. The aqueous GO dispersion was extensively washed and filtered with 1 M HCl and was then dialyzed with a dialysis membrane (Spectra Dialysis Membrane, MWCO: 6 ~ 8000) for 7 days to remove the salt byproduct and excess acid. Dried GO powder was dissolved in DI water at a concentration of 0.2 wt%. Then, an ammonia solution was added to the GO suspension until pH value becomes 11. After adding 1 mL of H_2O_2, GO solution underwent a hydrothermal treatment in a sealed Teflon vessel in an autoclave for 5 hours at 150 °C. After the synthetic reaction of the GQDs, the solution was filtered with a PTFE membrane (Millipore, pore size: 100 nm). The pH value of resulting clear solution was 8.3.

2.3. Fabrication of TiO_2 hollow nanowire array

The TiO_2 hollow nanowires have already demonstrated to be promising architectures for solar energy conversion applications, due to the promotion of light scattering effects, which leads to enhanced light harvesting efficiency.[6a] In the present study, we synthesized these structures by using ZnO nanowire templates.[6a] The zinc oxide (ZnO) film of 200 nm was deposited on FTO substrate using radio frequency magnetron sputtering. Vertically aligned ZnO nanorods array were grown on the ZnO seed layer coated FTO substrate via hydrothermal method. TiO_2 layer was coated on the ZnO nanorod template, and then ZnO was etched out in boric acid solution. These ZnO nanorods only serve as template to generate the hollow TiO_2 nanowires and do not have any functional role in the device. Details are well described on our previous study [6]. TiO_2 HNW array was calcined at 500 °C for 0.5 h under Ar atmosphere to obtain anatase phase TiO_2.

2.4. Decorating TiO_2 hollow nanowire with graphene quantum dots

The resultant GQDs 0.005 g was dispersed in 4 ml of ultrapure deionized water. Then, the TiO_2 HNW electrode was placed in the GQDs solution overnight. The GQDs are uniformly decorated on

TiO_2 due to electrostatic attraction between TiO_2 and GQD and the white color TiO_2 electrode turned light brownish. Finally the GQD decorated TiO_2 was washed with pure water and dried at N atmosphere.

2.5. Characterization techniques

The photoluminescence (PL) emission was recorded using Dongwoo Optron Co. Ltd. PL spectroscopy. The samples were irradiating at ambient temperature with a HeCd laser source (IK3501R-G, 325 nm). The beam width and resolution was controlled by MonoRa-750i Monochromator. The whole system equipped with a data acquisition unit (DAQ), a digitizer DAD-1602U, and optics for guiding the excitation beam and collecting luminescence signals. The optical absorbance measurements were carried out using JASCO 570 spectrophotometer. Structural morphology of the samples was studied using a JEOL JEM-3100F field emission scanning electron microscope (SEM) and a JEOL JSM 7600F field emission transmission electron microscope (TEM). Steady state current density voltage (j-V), measurements were carried out using a FRA equipped PGSTAT-30 from Autolab. A three-electrode configuration was used, where the G-QD/TiO_2 photo-electrode was connected to the working electrode, a Pt wire was connected to the counter electrode and a saturated Ag/AgCl was used as the reference electrode. The aqueous solution (0.5 M) of Na_2SO_4 was used as the electrolyte. In order to avoid the presence of oxygen (electron acceptor) in the solution, the electrolyte was bubbled with nitrogen gas for 30 min. The pH of the solution was 5.9 and all the electrochemical measurements were referred to the reversible hydrogen electrode (RHE) by the equation $V_{RHE} = V\ Ag/AgCl + 0.197 + pH\ (0.059)$. The electrodes were illuminated using a 300 W Xe lamp and the light intensity was adjusted with a thermopile to 100 mW/cm^2, with illumination through the substrate. EIS measurements were carried out in a three electrode configuration, applying 20 mV AC signal and scanning in a frequency range between 100 kHz and 0.1 Hz, at different applied biases. The IPCE measurements were carried out by employing a 300 W Xe lamp coupled with a computer-controlled monochromator; the photoelectrode was polarized at the desired voltage with a Gamry potentiostat, and the photocurrent was measured using an optical power meter 70310 from Oriel Instruments.

3. Results and discussion

The as-synthesized GQDs suspension from chemical exfoliation of graphene oxide exhibits a brownish colour as showed in Fig 1a and is dispersed in deionized water. Upon illumination with monochromatic UV light (365 nm), strong green fluorescence can be observed (Fig 1b). The PL spectrum ensures the visible light band gap excitation at GQDs. Further, the visible light activity of GQDs was verified with optical absorbance spectra, which clearly indicates the band edge falls above 450 nm (Fig. 1c). The size of the GQDs is analyzed with transmission electron microscopy (TEM) (Fig 1d) and shows a narrow size distribution with the average diameter of ~2 nm (Fig 1e). The structural morphology of the pristine TiO_2 thin films is showed in Fig 2a as vertically grown HNWS. The characteristic dimensions of the individual wires can be extracted from HRTEM micrographs (Fig 2b) and found to be ~3 μm in length and ~250 nm in diameter. After GQD sensitization (Fig 2c), the presence of carbon can be locally detected at the surface of the hollow nanowires through EDS analysis, see Fig 2d. However, the morphology of these GQDs cannot be clearly determined even at high magnification (Fig. 2c).

In order to further assess the presence of GQDs on TiO_2 HNWs, the optical absorbance of HNWs TiO_2 (A) was determined from transmittance (T) and diffuse reflectance (R) measurements using

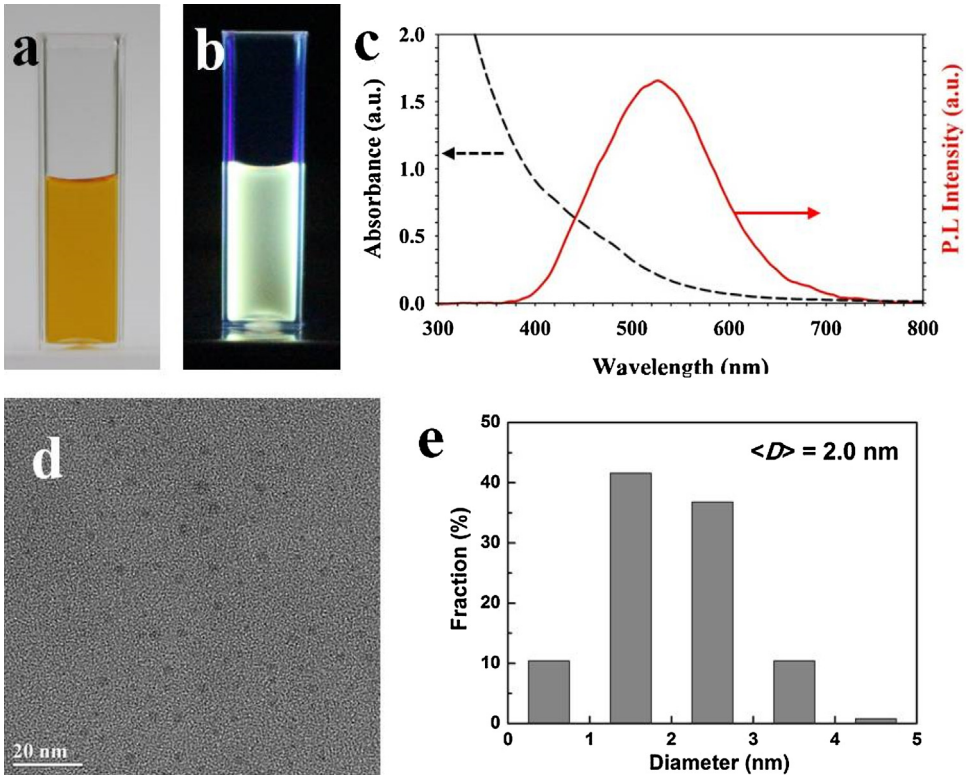

Fig. 1. (a) Photograph of GQDs solution under visible illumination and (b) under monochromatic light illumination (l_{exc} = 365 nm), (c) Photoluminesce and optical absorbance spectrum of GQDs solution (l_{exc} = 365 nm) (d) HRTEM image of GQD solution and (e) size distribution of GQDs estimated from Fig. 1d. (Consider changing "e" to black colour instead of red.)

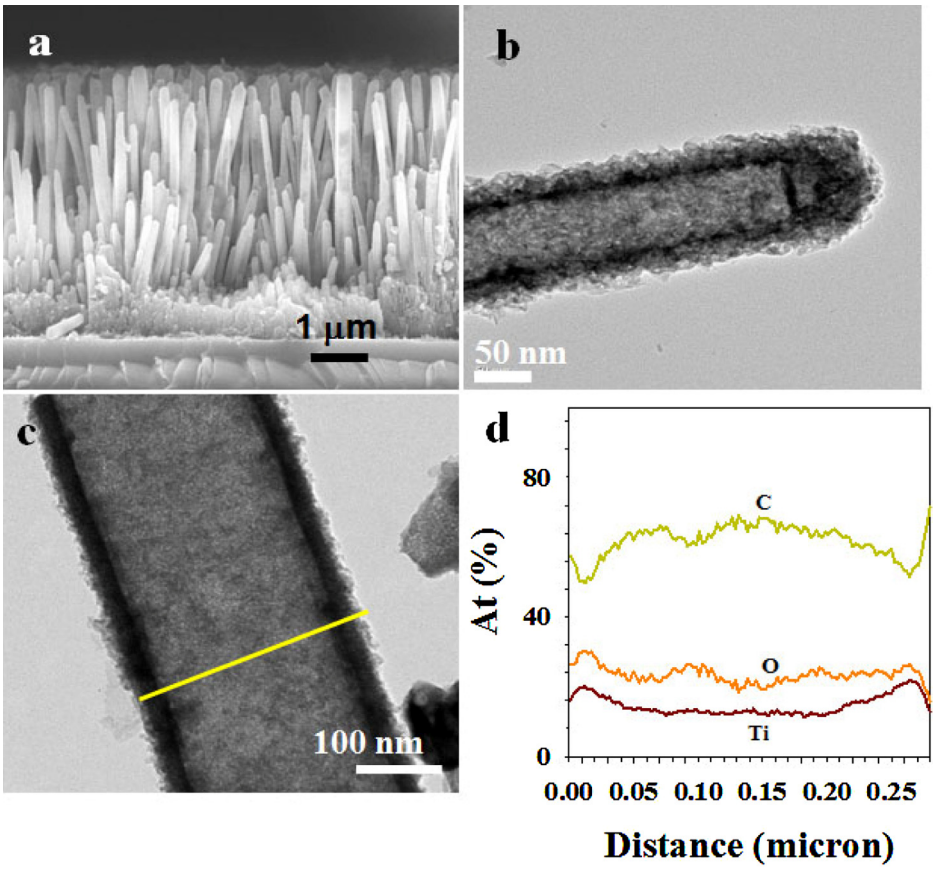

Fig. 2. (a) Cross section SEM image and (b) HRTEM image of pristine TiO_2 HNWs; (c) HRTEM image of GQDs-sensitized TiO_2 HNWs (elemental mapping results recorded across the TiO_2 HNWs indicated in different yellow color line) (d) Elemental mapping results.

the expression$A = -\log(T + R)$. The TiO_2 HNWs absorb light up to 400 nm, although a large absorption tail extending up to 600 nm exists due to scattering effects at the HNWs (Fig. 3). After GQD sensitization, the absorption is significantly enhanced both at the ultraviolet (UV) and visible regions of the electromagnetic spectrum. The high absorbance occurred at UV region is attributed to the π–π^* transition of aromatic sp^2 domains in GQDs [44]. The visible light absorption is originated from the excitation between σ and π orbital (HOMO) to the lowest unoccupied molecular orbital (LUMO) [45].

The photocharge carrier generation at GQDs and TiO_2 upon photoirradiation is schematically explained in Scheme 1. The charge transfer at heterostructured TiO_2-GQDs system can be qualitatively understood by the energy diagram showed in Scheme 1, where the conduction band position of the GQDs is more negative compared to that of TiO_2.[15] Therefore, both materials are aligned in a type II configuration and consequently photogenerated holes at the GQDs can be injected to the solution

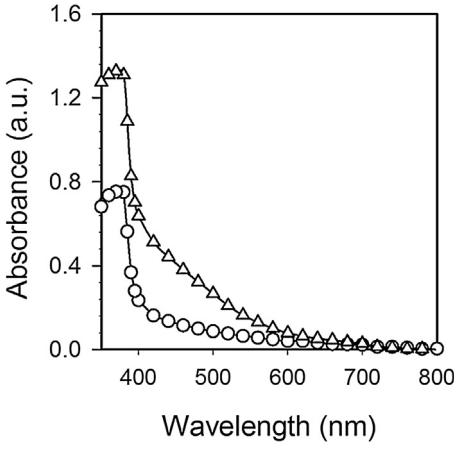

Fig. 3. Optical absorbance spectra of pristine and GQDs coated TiO_2 electrode. (the symbol indicated 'Δ' represents pristine TiO_2 and 'Δ' indicates GQDs sensitized TiO_2).

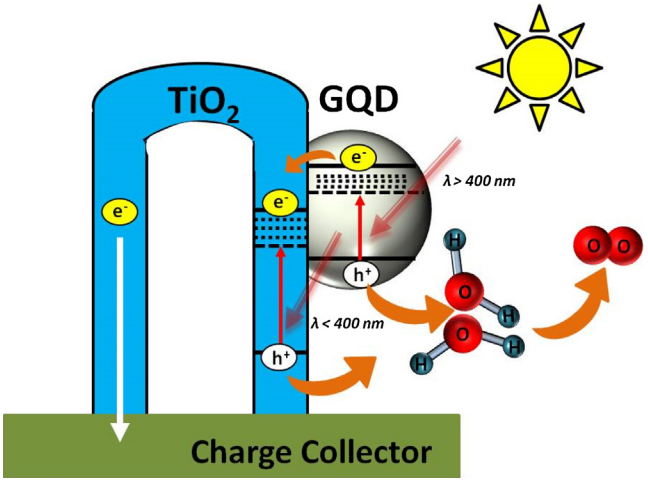

Scheme 1. Photoexcitation charge carriers generated at GQDs/TiO_2 interfaces. The photoholes from valence band of GQD and TiO_2 involves in water oxidation phenomena and produce oxygen gas molecules. The electrons from conduction band of GQD and TiO_2 will transport to charge collector.

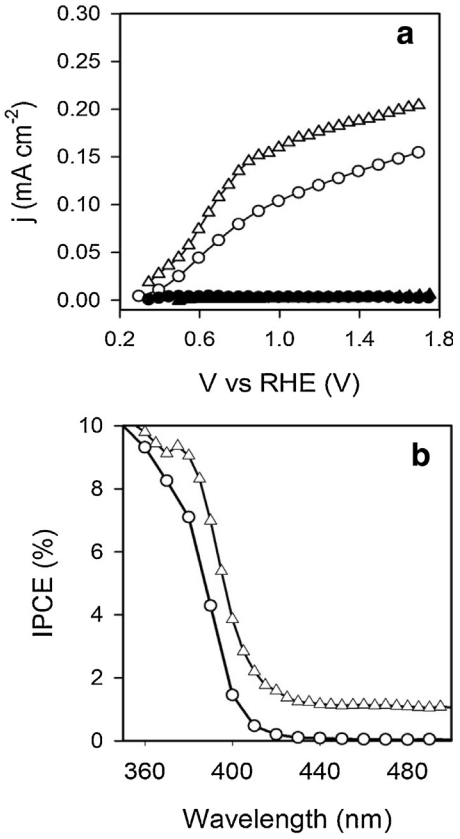

Fig. 4. (a) j-V curves and (b) IPCE spectra at 1.23 V vs RHE of pristine TiO_2 nanowires and after sensitization with GQDs (the symbol indicated 'Δ' represents pristine TiO_2 and 'Δ' indicates GQDs sensitized TiO_2).

(water oxidation), while photogenerated electrons are injected into TiO_2, and then to the contact (charge collector). This energy diagram scheme is consistent with previous studies with carbon quantum dots.[16] According to this energy diagram scheme, the measured photocurrents can be related to water oxidation. The enhanced optical absorption at the hybrid nanocomposite films leads to higher photocurrents for water oxidation, as showed in Fig 4a. At 1.23 V vs RHE, pristine TiO_2 HNWs deliver a photocurrent of 0.12 mA cm^{-2}, while 0.18 mA cm^{-2} are obtained after GQDs sensitization.

The possibility of light scattering from GQDs may also enhance optical path ways of TiO_2. However, it is noticed that the reflectance of TiO_2 is found to reduce from 400-500 nm wavelength after decorating GQDs (See supporting information Fig. S1). This implies that GQDs could absorb the light photons at 400-500 nm wavelengths. Further the photocurrent enhancement at TiO_2 by GQDs is examined with external quantum efficiency analysis. Fig. 4b, the IPCE spectra clearly evidence that this enhancement is due to the extension of the optical absorption of the heterostructure.

A contribution of scattering to the photocurrent after GQDs sensitization is also deduced from the flat IPCE signal above 450 nm. Integration of the IPCE spectra obtained at 1.23 V vs RHE with the solar spectrum leads to photocurrent values very close to those observed in the j-V curves of Fig. 4a (0.12 mA · cm^{-2} and 0.19 mA · cm^{-2} for TiO_2 and TiO_2-GQDs, respectively). At this stage, optimization of the GQDs loading onto TiO_2 HNWs is needed to significantly enhance the device performance targeting competitive efficiencies.

Further insight into the optoelectronic and photoelectrochemical behaviour showed in Fig. 4 can be gained on the basis of physical modelling fed by results provided by impedance spectroscopy. The experimental impedance spectra (Nyquist plots) systematically showed a single arc in the dark and under illumination for all applied voltages (Fig. 5a and b) and consequently, we used the simple equivalent circuit showed in Fig. 5c, to fit these spectra. The electrical elements of the selected equivalent circuit included a series resistance (R_s) accounting for the resistance at the contacts and wiring elements connected in series with the parallel combination of a charge transfer resistance (R_{ct}), which describes the charge transfer kinetics of electrons

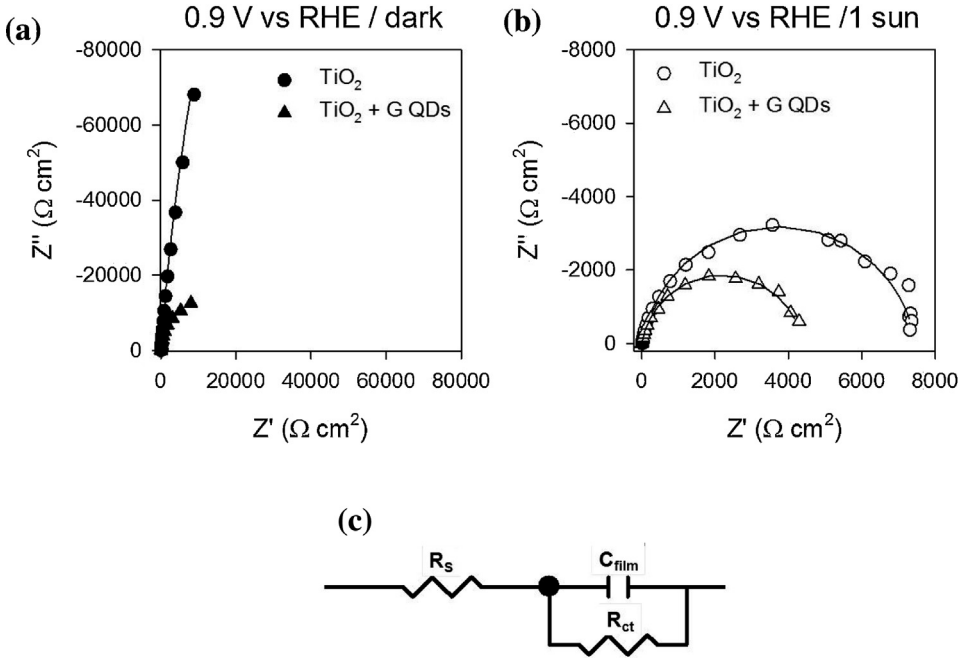

Fig. 5. Representative Nyquist plots of the impedance spectra obtained on the tested samples in 0.5 M Na_2SO_4 solution in the (a) dark and (b) under illumination; (c) electrical equivalent circuit used for fitting the impedance response data of the tested materials.

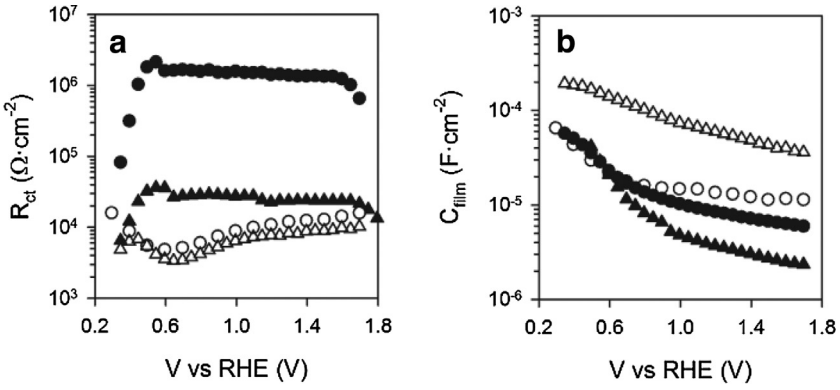

Fig. 6. (a) Charge transfer resistance and (b) Film capacitance on bare TiO_2 (circles) and GQD decorated TiO_2 electrodes (triangles) in the dark (black) and under illumination (100 mW cm^{-2}) conditions (white).

recombining with the surface states/species in solution and a capacitance (C_{film}), which conveys information of charge accumulation mechanisms at the semiconductor/solution interface. The estimated charge capacitance (C_{film}) from equivalent circuit analysis is presented at different scale in Fig. S2 (a, b and c).

Fig. 6 compiles the most relevant results for R_{ct} and C_{film}. The charge transfer kinetics is systematically faster for TiO_2-GQDs samples as evidenced by the higher charge transfer resistance found for the pristine TiO_2 architecture (Fig. 6a). Both, j-V curves and R_{ct} in the dark show increased recombination for TiO_2-GQDs. On the other hand, the capacitance in the dark (Fig. 6b) shows the characteristic exponential dependence on voltage previously reported for the distribution of interbandgap states in TiO_2, for both specimens below 0.8 V versus RHE.[17] At more positive potentials, the capacitive signatures are dominated by the FTO substrate and the reasons for the different values are related to the exposure of the substrate to the solution, (see Fig. S1 Mott-Schottky plots). The cyclic voltammetry curves before and after impedance spectroscopy measurements were very similar indicating that the films are stable for at least 2 hours under operation.

Under illumination, the chemical capacitance of TiO_2 is identical to that in the dark, since this capacitance is mainly governed by the applied bias that controls the Fermi level of TiO_2 HNWs. Under illumination, the resultant photoinduced charge accumulation at the GQDs (white triangles in Fig. 7b) is believed to be the reason for the significantly increased capacitance at all applied potentials. The possible mechanism of the observed photoinduced charge accumulation at GQDs/TiO_2 can be explained on the basis of Long et al. [22], i.e.: GQDs can be chemisorbed onto TiO_2 (110) surface through the O-Ti covalent bonds.

As it is discussed above, photoexcited electrons generated at the GQD enhance the charge density. This enhancement is reflected on the decreased R_{ct} under illumination (Fig. 6a). However the much larger difference in the capacitance of TiO_2-GQDs compared to the small change in R_{ct} suggests that recombination kinetics of GQDs under illumination is slowed down compared to pristine TiO_2.

4. Conclusion

In conclusion, we have prepared colloidal GQDs as effective sensitizers of TiO_2 hollow nanowires for enhancing the light harvesting efficiency and the catalytic activity for water oxidation of this material providing a promising demonstration of concept of hybrid architecture for water photo-oxidation, without the need of sacrificial agents (hole scavengers). Due to their enhanced properties, these heterostructures outperform pristine TiO_2 electrodes, although water oxidation photocurrents must be significantly increased in order to attain reasonable energy conversion efficiencies for technological exploitation. The impedance analysis on TiO_2-GQDs provides a platform to understand the energetic structure of heterophotocatalytic interfaces at working condition. It is anticipated that this impedance model can be further implemented in GQDs based solar light driven devices, where GQDs perform as electron transporter or photosensitizers [46,11,47,22,48]. In particular, the interrelationship between charge capacitance and charge transfer resistance at metal oxide-GQDs interfaces will be informative of the control the recombination rate at photoelectrochemical fuel generation systems.

Acknowledgment

This research was supported by Basic Science Research Program through the National Research Foundation of Korea (NRF 2014R1A1A1008196). The author PS (ID: P13374) are highly grateful to the “Japan Society for the Promotion of Science (JSPS) Postdoctoral Fellowship Program for Foreign Researchers” for the financial assistance. This work was also supported by the Korea Center for Artificial Photosynthesis (KCAP) located in Sogang University funded through the National Research Foundation of Korea (No. 2009-0093883).

Appendix A. Supplementary data

Supplementary data associated with this article can be found, in the online version, at http://dx.doi.org/10.1016/j.electacta.2015.11.048.

References

[1] M.G. Walter, E.L. Warren, J.R. McKone, S.W. Boettcher, Q.X. Mi, E.A. Santori, N.S. Lewis, Solar Water Splitting Cells, Chemical Reviews 110 (2010) 6446–6473.
[2] A. Fujishima, K. Honda, Electrochemical photolysis of water at semiconductor electrode, Nature 238 (1972) 37–38.
[3] S.U.M. Khan, M. Al-Shahry, W.B. Ingler, Efficient photochemical water splitting by a chemically modified n-TiO_2, Science 297 (2002) 2243–2245.
[4] R. Asahi, T. Morikawa, T. Ohwaki, K. Aoki, Y. Taga, Visible-light photocatalysis in nitrogen-doped titanium oxides, Science 293 (2001) 269–271.
[5] T. Umebayashi, T. Yamaki, H. Itoh, K. Asai, Band gap narrowing of titanium dioxide by sulfur doping, Applied Physics Letters 81 (2002) 454–456.
[6] P. Rodenas, T. Song, P. Sudhagar, G. Marzari, H. Han, L. Badia-Bou, S. Gimenez, F. Fabregat-Santiago, I. Mora-Sero, J. Bisquert, U. Paik, Y.S. Kang, Quantum Dot Based Heterostructures for Unassisted Photoelectrochemical Hydrogen Generation, Advanced Energy Materials 3 (2013) 176–182.
[7] R. Trevisan, P. Rodenas, V. Gonzalez-Pedro, C. Sima, R.S. Sanchez, E.M. Barea, I. Mora-Sero, F. Fabregat-Santiago, S. Gimenez, Harnessing Infrared Photons for Photoelectrochemical Hydrogen Generation. A PbS Quantum Dot Based Quasi-Artificial Leaf, The Journal of Physical Chemistry Letters 4 (2012) 141–146.

[8] V. Gonzalez-Pedro, I. Zarazua, E.M. Barea, F. Fabregat-Santiago, E. de la Rosa, I. Mora-Sero, S. Gimenez, Panchromatic Solar-to-H-2Conversion by a Hybrid Quantum Dots-Dye Dual Absorber Tandem Device, Journal of Physical Chemistry C 118 (2014) 891–895.
[9] K.S. Novoselov, A.K. Geim, S.V. Morozov, D. Jiang, Y. Zhang, S.V. Dubonos, I.V. Grigorieva, A.A. Firsov, Electric field effect in atomically thin carbon films, Science 306 (2004) 666–669.
[10] X. Yan, X. Cui, B. Li, L.-s. Li, Large, Solution-Processable Graphene Quantum Dots as Light Absorbers for Photovoltaics, Nano Letters 10 (2010) 1869–1873.
[11] Z. Zhu, J. Ma, Z. Wang, C. Mu, Z. Fan, L. Du, Y. Bai, L. Fan, H. Yan, D.L. Phillips, S. Yang, Efficiency Enhancement of Perovskite Solar Cells through Fast Electron Extraction: The Role of Graphene Quantum Dots, Journal of the American Chemical Society 136 (2014) 3760–3763.
[12] F. Schedin, A.K. Geim, S.V. Morozov, E.W. Hill, P. Blake, M.I. Katsnelson, K.S. Novoselov, Detection of individual gas molecules adsorbed on graphene, Nature Materials 6 (2007) 652–655.
[13] G.C. Xie, K. Zhang, B.D. Guo, Q. Liu, L. Fang, J.R. Gong, Graphene-Based Materials for Hydrogen Generation from Light-Driven Water Splitting, Advanced Materials 25 (2013) 3820–3839.
[14] M.L. Mueller, X. Yan, J.A. McGuire, L.S. Li, Triplet States and Electronic Relaxation in Photoexcited Graphene Quantum Dots, Nano Letters 10 (2010) 2679–2682.
[15] D. Pan, J. Zhang, Z. Li, M. Wu, Hydrothermal Route for Cutting Graphene Sheets into Blue-Luminescent Graphene Quantum Dots, Advanced Materials 22 (2010) 734–738.
[16] Q. Xue, H. Huang, L. Wang, Z. Chen, M. Wu, Z. Li, D. Pan, Nearly monodisperse graphene quantum dots fabricated by amine-assisted cutting and ultrafiltration, Nanoscale 5 (2013) 12098–12103.
[17] A. Ananthanarayanan, X. Wang, P. Routh, B. Sana, S. Lim, D.-H. Kim, K.-H. Lim, J. Li, P. Chen, Facile Synthesis of Graphene Quantum Dots from 3D Graphene and their Application for Fe3+ Sensing, Advanced Functional Materials 24 (2014) 3021–3026.
[18] Y. Shin, J. Lee, J. Yang, J. Park, K. Lee, S. Kim, Y. Park, H. Lee, Mass Production of Graphene Quantum Dots by One-Pot Synthesis Directly from Graphite in High Yield, Small 10 (2014) 866–870.
[19] W. Kwon, Y.-H. Kim, C.-L. Lee, M. Lee, H.C. Choi, T.-W. Lee, S.-W. Rhee, Electroluminescence from Graphene Quantum Dots Prepared by Amidative Cutting of Tattered Graphite, Nano Letters 14 (2014) 1306–1311.
[20] Y. Sun, S. Wang, C. Li, P. Luo, L. Tao, Y. Wei, G. Shi, Large scale preparation of graphene quantum dots from graphite with tunable fluorescence properties, Physical Chemistry Chemical Physics 15 (2013) 9907–9913.
[21] Y. Liu, B. Gao, Z. Qiao, Y. Hu, W. Zheng, L. Zhang, Y. Zhou, G. Ji, G. Yang, Gram-Scale Synthesis of Graphene Quantum Dots from Single Carbon Atoms Growth via Energetic Material Deflagration, Chemistry of Materials (2015) .
[22] R. Long, Understanding the Electronic Structures of Graphene Quantum Dot Physisorption and Chemisorption onto the TiO2 (110) Surface: A First-Principles Calculation, ChemPhysChem 14 (2013) 579–582.
[23] L. Wang, Y. Wang, T. Xu, H. Liao, C. Yao, Y. Liu, Z. Li, Z. Chen, D. Pan, L. Sun, M. Wu, Gram-scale synthesis of single-crystalline graphene quantum dots with superior optical properties, Nat Commun 5 (2014) .
[24] R. Ye, C. Xiang, J. Lin, Z. Peng, K. Huang, Z. Yan, N.P. Cook, E.L.G. Samuel, C.-C. Hwang, G. Ruan, G. Ceriotti, A.-R.O. Raji, A.A. Martí, J.M. Tour, Coal as an abundant source of graphene quantum dots, Nat Commun 4 (2013) .
[25] R. Ye, Z. Peng, A. Metzger, J. Lin, J.A. Mann, K. Huang, C. Xiang, X. Fan, E.L.G. Samuel, L.B. Alemany, A.A. Martí, J.M. Tour, Bandgap Engineering of Coal-Derived Graphene Quantum Dots, ACS Applied Materials & Interfaces 7 (2015) 7041–7048.
[26] P. Roy, A.P. Periasamy, C. Chuang, Y.-R. Liou, Y.-F. Chen, J. Joly, C.-T. Liang, H.-T. Chang, Plant leaf-derived graphene quantum dots and applications for white LEDs, New Journal of Chemistry 38 (2014) 4946–4951.
[27] T.S. Sreeprasad, A.A. Rodriguez, J. Colston, A. Graham, E. Shishkin, V. Pallem, V. Berry, Electron-Tunneling Modulation in Percolating Network of Graphene Quantum Dots: Fabrication, Phenomenological Understanding, and Humidity/Pressure Sensing Applications, Nano Letters 13 (2013) 1757–1763.
[28] H. Sun, L. Wu, W. Wei, X. Qu, Recent advances in graphene quantum dots for sensing, Materials Today 16 (2013) 433–442.
[29] J. Soong Sin, K. Jungkil, K. Soo Seok, K. Sung, C. Suk-Ho, H. Sung Won, Graphene-quantum-dot nonvolatile charge-trap flash memories, Nanotechnology 25 (2014) 255203.
[30] Y. Li, Y. Hu, Y. Zhao, G. Shi, L. Deng, Y. Hou, L. Qu, An Electrochemical Avenue to Green-Luminescent Graphene Quantum Dots as Potential Electron-Acceptors for Photovoltaics, Advanced Materials 23 (2011) 776–780.
[31] V. Gupta, N. Chaudhary, R. Srivastava, G.D. Sharma, R. Bhardwaj, S. Chand, Luminscent Graphene Quantum Dots for Organic Photovoltaic Devices, Journal of the American Chemical Society 133 (2011) 9960–9963.
[32] X. Yan, X. Cui, L.-s. Li, Synthesis of Large, Stable Colloidal Graphene Quantum Dots with Tunable Size, Journal of the American Chemical Society 132 (2010) 5944–5945.
[33] K. Lingam, R. Podila, H. Qian, S. Serkiz, A.M. Rao, Evidence for Edge-State Photoluminescence in Graphene Quantum Dots, Advanced Functional Materials 23 (2013) 5062–5065.
[34] J. Shen, Y. Zhu, X. Yang, C. Li, Graphene quantum dots: emergent nanolights for bioimaging, sensors, catalysis and photovoltaic devices, Chemical Communications 48 (2012) 3686–3699.
[35] J. Ge, M. Lan, B. Zhou, W. Liu, L. Guo, H. Wang, Q. Jia, G. Niu, X. Huang, H. Zhou, X. Meng, P. Wang, C.-S. Lee, W. Zhang, X. Han, A graphene quantum dot photodynamic therapy agent with high singlet oxygen generation, Nat Commun 5 (2014) .
[36] C.X. Guo, Y. Dong, H.B. Yang, C.M. Li, Graphene Quantum Dots as a Green Sensitizer to Functionalize ZnO Nanowire Arrays on F-Doped SnO2 Glass for Enhanced Photoelectrochemical Water Splitting, Advanced Energy Materials 3 (2013) 997–1003.
[37] Q. Zhang, J. Jie, S. Diao, Z. Shao, Q. Zhang, L. Wang, W. Deng, W. Hu, H. Xia, X. Yuan, S.-T. Lee, Solution-Processed Graphene Quantum Dot Deep-UV Photodetectors, ACS Nano 9 (2015) 1561–1570.
[38] D. Pan, C. Xi, Z. Li, L. Wang, Z. Chen, B. Lu, M. Wu, Electrophoretic fabrication of highly robust, efficient, and benign heterojunction photoelectrocatalysts based on graphene-quantum-dot sensitized TiO2 nanotube arrays, Journal of Materials Chemistry A 1 (2013) 3551–3555.
[39] M. Dutta, S. Sarkar, T. Ghosh, D. Basak, ZnO/Graphene Quantum Dot Solid-State Solar Cell, The Journal of Physical Chemistry C 116 (2012) 20127–20131.
[40] K.J. Williams, C.A. Nelson, X. Yan, L.-S. Li, X. Zhu, Hot Electron Injection from Graphene Quantum Dots to TiO2, ACS Nano 7 (2013) 1388–1394.
[41] X. Wang, D. Ling, Y. Wang, H. Long, Y. Sun, Y. Shi, Y. Chen, Y. Jing, Y. Sun, Y. Dai, N-doped graphene quantum dots-functionalized titanium dioxide nanofibers and their highly efficient photocurrent response, Journal of Materials Research 29 (2014) 1408–1416.
[42] T.H. Han, Y.-K. Huang, A.T.L. Tan, V.P. Dravid, J. Huang, Steam Etched Porous Graphene Oxide Network for Chemical Sensing, Journal of the American Chemical Society 133 (2011) 15264–15267.
[43] T.H. Han, W.J. Lee, D.H. Lee, J.E. Kim, E.-Y. Choi, S.O. Kim, Peptide/Graphene Hybrid Assembly into Core/Shell Nanowires, Advanced Materials 22 (2010) 2060–2064.
[44] J. Peng, W. Gao, B.K. Gupta, Z. Liu, R. Romero-Aburto, L. Ge, L. Song, L.B. Alemany, X. Zhan, G. Gao, S.A. Vithayathil, B.A. Kaipparettu, A.A. Marti, T. Hayashi, J.-J. Zhu, P.M. Ajayan, Graphene Quantum Dots Derived from Carbon Fibers, Nano Letters 12 (2012) 844–849.
[45] H. Riesen, C. Wiebeler, S. Schumacher, Optical Spectroscopy of Graphene Quantum Dots: The Case of C132, The Journal of Physical Chemistry A 118 (2014) 5189–5195.
[46] P. Gao, K. Ding, Y. Wang, K. Ruan, S. Diao, Q. Zhang, B. Sun, J. Jie, Crystalline Si/Graphene Quantum Dots Heterojunction Solar Cells, The Journal of Physical Chemistry C 118 (2014) 5164–5171.
[47] M. Sun, S. Qu, W. Ji, P. Jing, D. Li, L. Qin, J. Cao, H. Zhang, J. Zhao, D. Shen, Towards efficient photoinduced charge separation in carbon nanodots and TiO2 composites in the visible region, Physical Chemistry Chemical Physics 17 (2015) 7966–7971.
[48] H. Li, J. Xing, Z. Xia, J. Chen, Preparation of coaxial heterogeneous graphene quantum dot-sensitized TiO2 nanotube arrays via linker molecule binding and electrophoretic deposition, Carbon 81 (2015) 474–487.